New Solitary-Wave Solutions for the Generalized Reaction Duffing Model and their Dynamics

Jong-Jae Kim and Woo-Pyo Hong

Department of Physics, Catholic University of Daegu, Hayang, Kyongsan, Kyungbuk 712-702, South Korea

Reprint requests to Prof. W.-P. H.; E-mail: wphong@as.ac.kr

Z. Naturforsch. **59a,** 721 – 728 (2004); received June 2, 2004

We find new analytic solitary-wave solutions, having a nonzero background at infinity, of the generalized reaction Duffing model using the auxiliary function method. We study the dynamical properties of the solitary-waves by numerical simulations. It is shown that the solitary-waves can be stable or unstable depending on the coefficients of the model. We study the interaction dynamics by using the solitary-waves as initial profiles to show that the nonlinear terms may act as an effective driving force. – PACS numbers: 03.40.Kf, 02.30.Jr, 47.20.Ky, 52.35.Mw

Key words: Generalized Reaction Duffing Model; Analytic Solitary-Wave Solutions; Numerical Simulation; Stability; Interaction.

1. Introduction

As a generalized nonlinear evolution equation including such famous ones as the Klein-Gordon, Landau-Ginzburg-Higgs and ϕ^4 equations [1 – 3], we consider the generalized reaction Duffing equation

$$v_{tt} + \alpha v_{xx} + \beta v + \gamma v^2 + \delta v^3 = 0, \tag{1}$$

where α, β, γ, and δ are constants. Several solitary-wave and periodic solutions of (1) have been found by Yan and Zhang [4, 5]. More recently, Tian and Gao [6] have reported several families of exact solitonic solutions, including the shock and bell-shaped waves.

The purpose of this paper is to investigate new analytic solitary-wave solutions for (1) by using the auxiliary differential equation method [7, 8] and investigate their dynamical behaviors. In Sect. 2, we introduce the auxiliary differential equation method for finding the solitary-wave solutions and investigate the coefficients region for such solutions. In Sect. 3, we investigate the dynamics of the solitary-waves using a numerical method. The conclusions are in Section 4.

2. The Auxiliary Equation Method and Analytic Solitary-Wave Solutions

In this section, we first describe the auxiliary equation method [7, 8]. Suppose we are given a nonlinear partial differential equation (NLPDE) for $v(x,t)$ in the form

$$H(v, v_x, v_t, v_{xx}, v_{tt}, v_{xt} \ldots) = 0. \tag{2}$$

Introducing the similarity variable $\xi = x - \lambda t$, the traveling wave solution of $v(\xi)$ satisfies the ODE

$$G(v, v_\xi, v_{\xi\xi}, v_{\xi\xi\xi}, \ldots) = 0. \tag{3}$$

By virtue of the extended tanh-function method one assumes that the solution of (3) has the form

$$v(\xi) = \sum_{i=0}^{n} a_i z^i(\xi), \tag{4}$$

in which a_i ($i = 1, 2, \ldots, n$), λ are all real constants to be determined, the order n is a positive integer which can be readily determined by balancing the highest order derivative term with the highest power nonlinear term in (3), and $z(\xi)$ expresses the solutions of the following auxiliary ordinary differential equation

$$\left(\frac{\mathrm{d}z}{\mathrm{d}\xi}\right)^2 = az^2(\xi) + bz^3(\xi) + cz^4(\xi), \tag{5}$$

where a, b, and c are real parameters. We seek the exact solutions of (3) by using the following solutions of (5):

0932–0784 / 04 / 1100–0721 $ 06.00

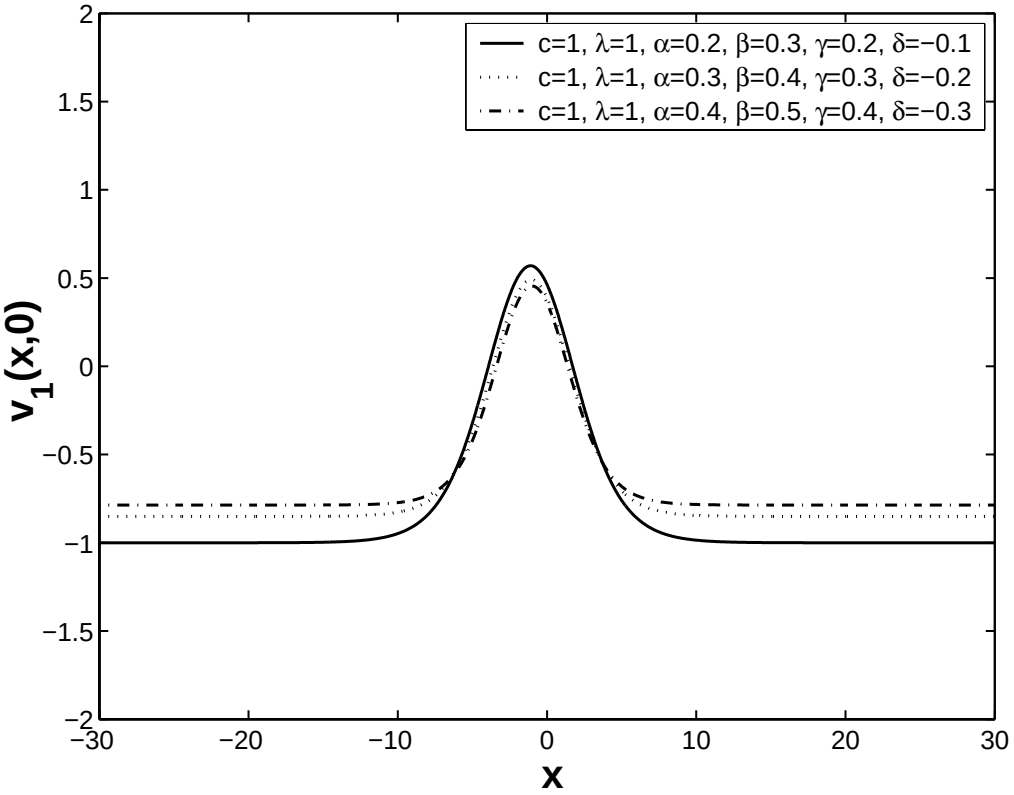

Fig. 1. The profile of bright solitary-wave type solution $v_1(x,0)$ for different model coefficients which satisfy the constraint $a>0$. As the strength of the higher nonlinear terms increase, the width and amplitude of the solitary-wave decrease.

$$z(\xi)=\begin{cases}\dfrac{-ab\,\mathrm{sech}^2(\pm\frac{\sqrt{a}}{2}\xi)}{b^2-ac\,(1-\tanh(\pm\frac{\sqrt{a}}{2}\xi))^2}, & \text{when } a>0,\\ \dfrac{2a\,\mathrm{sech}(\sqrt{a}\xi)}{\sqrt{b^2-4ac}-b\,\mathrm{sech}(\sqrt{a}\xi)}, & \\ \text{when}\sqrt{b^2-4ac}>0 \text{ and } a>0.\end{cases} \tag{6}$$

To look for the traveling wave solutions of (1), we consider the transformation $v(x,t)=v(\xi)$, leading to

$$(\alpha+\lambda^2)v_{\xi\xi}+\delta v^3+\beta v+\gamma v^2=0. \tag{7}$$

By balancing the highest order derivative $v_{\xi\xi}$ with the highest power nonlinear term v^3 yields $n=1$. Therefore, we choose a solution of (1) in the form

$$v(\xi)=a_0+a_1 z(\xi), \tag{8}$$

where a_0 and a_1 are constants to be determined. By substituting (5) and (8) into (7) and setting the coefficients of $z^j(\xi)(j=0,1,2,..,7)$ to zero, we find a set of algebraic equations for a,b,c,a_0,a_1, and λ:

$$\begin{aligned}
&\gamma a_0+\beta+\delta {a_0}^2=0,\\
&b\gamma {a_0}^2+b\beta a_0+b\delta {a_0}^3+a_1\alpha a^2+3a\delta {a_0}^2 a_1\\
&\quad +a\beta a_1+2a\gamma a_0 a_1+a_1\lambda^2 a^2=0,\\
&c\gamma {a_0}^2+c\beta a_0+c\delta {a_0}^3+\frac{5}{2}ba_1\alpha a+3b\delta {a_0}^2 a_1\\
&\quad +b\beta a_1+2b\gamma a_0 a_1+\frac{5}{2}ba_1\lambda^2 a+a\gamma {a_1}^2\\
&\quad +3a\delta a_0 {a_1}^2=0,\\
&6c\alpha a+6c\delta {a_0}^2+2\beta c+4c\gamma a_0+6c\lambda^2 a+2a_1 b\gamma\\
&\quad +3\alpha b^2+3\lambda^2 b^2+6a_1 b\delta a_0+2{a_1}^2 a\delta=0,\\
&2a_1 c\gamma+7c\alpha b+7c\lambda^2 b+6a_1 c\delta a_0+2{a_1}^2 b\delta=0,\\
&2\lambda^2 c+2\alpha c+\delta {a_1}^2 c=0.
\end{aligned} \tag{9}$$

By solving these overdetermined algebraic equations, we obtain

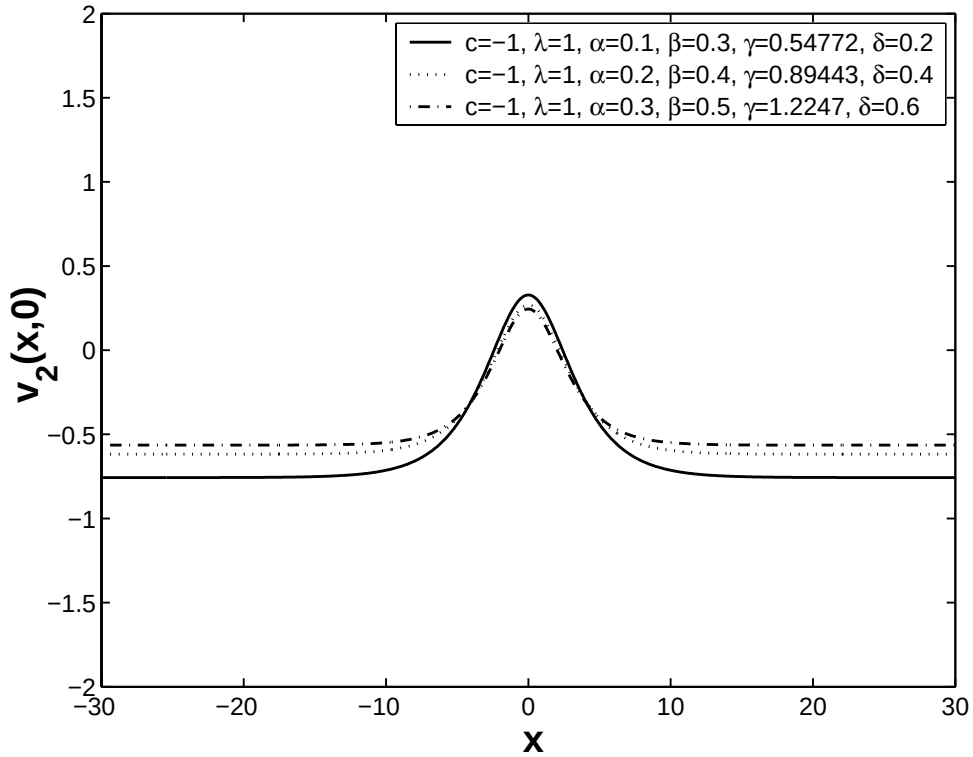

Fig. 2. The profile of bright solitary-wave type solution $v_2(x,0)$ for different model coefficients which satisfy the constraints $a>0$ and $\sqrt{b^2-4ac}>0$. As the strength of the higher nonlinear terms increase, the width and amplitude of the solitary-wave decrease.

Case 1

$$a=\frac{-\gamma^2+\gamma\sqrt{\gamma^2-4\delta\beta}+4\delta\beta}{2\delta(\alpha+\lambda^2)},$$
$$b=\frac{\sqrt{2}}{3}\frac{(-\gamma+3\sqrt{\gamma^2-4\delta\beta})c}{\sqrt{-\delta c(\alpha+\lambda^2)}},$$
$$a_0=\frac{-\gamma+\sqrt{\gamma^2-4\delta\beta}}{2\delta},$$
$$a_1=\frac{\sqrt{-2\delta c(\alpha+\lambda^2)}}{\delta}. \tag{10}$$

Case 2

$$a=\frac{-\gamma^2-\gamma\sqrt{\gamma^2-4\delta\beta}-4\delta\beta}{2\delta(\alpha+\lambda^2)},$$
$$b=\frac{\sqrt{2}}{3}\frac{(\gamma+3\sqrt{\gamma^2-4\delta\beta})c}{\sqrt{-\delta c(\alpha+\lambda^2)}},$$
$$a_0=\frac{-\gamma-\sqrt{\gamma^2-4\delta\beta}}{2\delta},$$
$$a_1=-\frac{\sqrt{-2\delta c(\alpha+\lambda^2)}}{\delta}. \tag{11}$$

Case 3

$$a=\frac{-\gamma^2+\gamma\sqrt{\gamma^2-4\delta\beta}+4\delta\beta}{2\delta(\alpha+\lambda^2)},$$
$$b=\frac{\sqrt{2}}{3}\frac{(\gamma-3\sqrt{\gamma^2-4\delta\beta})c}{\sqrt{-\delta c(\alpha+\lambda^2)}},$$
$$a_0=\frac{-\gamma+\sqrt{\gamma^2-4\delta\beta}}{2\delta},$$
$$a_1=-\frac{\sqrt{-2\delta c(\alpha+\lambda^2)}}{\delta}. \tag{12}$$

Case 4

$$a=\frac{-\gamma^2-\gamma\sqrt{\gamma^2-4\delta\beta}-4\delta\beta}{2\delta(\alpha+\lambda^2)},$$
$$b=\frac{\sqrt{2}}{3}\frac{(-\gamma-3\sqrt{\gamma^2-4\delta\beta})c}{\sqrt{-\delta c(\alpha+\lambda^2)}},$$
$$a_0=\frac{-\gamma-\sqrt{\gamma^2-4\delta\beta}}{2\delta},$$
$$a_1=\frac{\sqrt{-2\delta c(\alpha+\lambda^2)}}{\delta}. \tag{13}$$

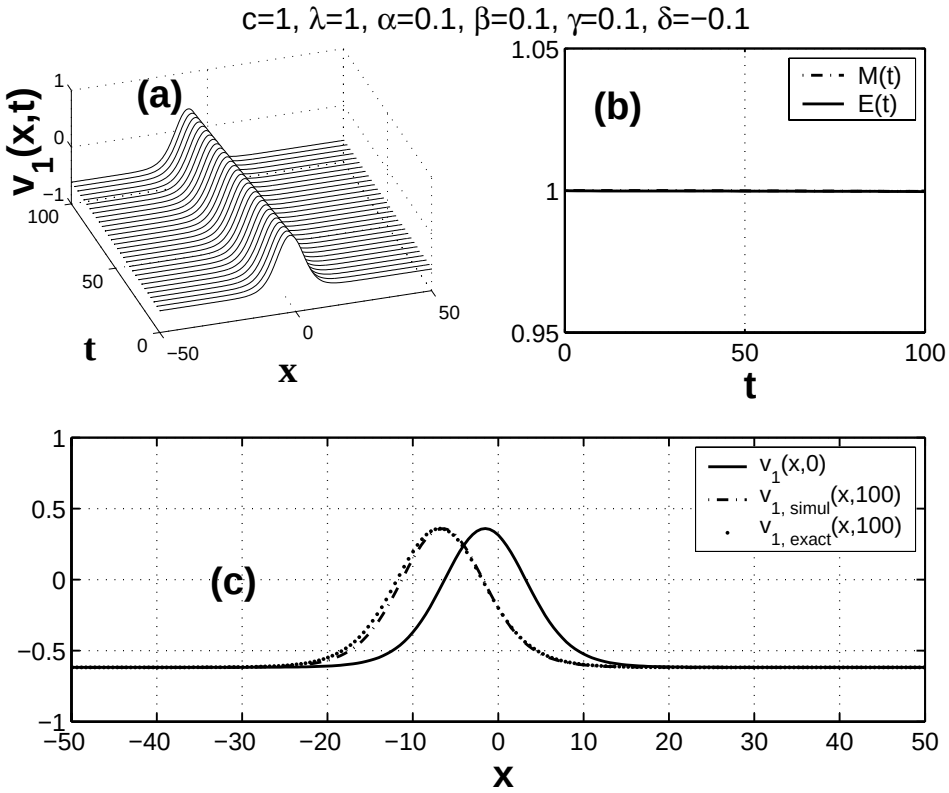

Fig. 3. a) Evolution of numerically simulated $v_1(x,t)$. b) Zero deviation from the initial values of the normalized mass and energy $M(t)$ and $E(t)$, respectively, indicates the stability of the solitary-wave. c) Comparison of the numerically simulated wave profile at $t = 100$ with that of the exact solitary-wave solution in (14), showing stable propagation along the evolution time.

According to (10)–(13), (8) and (6), we find new eight analytic solitary-wave solutions of (1) with the wavelength λ as a free parameter for the model. We note that the model coefficients $(\alpha,\beta,\gamma,\delta)$ can be further constrained by an auxiliary condition in (6), i.e., $a>0$ or $\sqrt{b^2-4ac}>0$ and $a>0$. As an example, for Case 2 we have two solitary-wave solutions in form of

$$v_1(x,t) = \frac{-\gamma+\sqrt{\gamma^2-4\delta\beta}}{2\delta} - \frac{\sqrt{-2\delta c(\alpha+\lambda^2)}}{\delta}\frac{ab\,\mathrm{sech}^2(\frac{\sqrt{a}}{2}\xi)}{b^2-ac[1-\tanh(\frac{\sqrt{a}}{2}\xi)]^2}, \tag{14}$$

and

$$v_2(x,t) = \frac{-\gamma+\sqrt{\gamma^2-4\delta\beta}}{2\delta} - \frac{\sqrt{-2\delta c(\alpha+\lambda^2)}}{\delta}\frac{2a\,\mathrm{sech}(\sqrt{a}\xi)}{\sqrt{b^2-4ac}-b\,\mathrm{sech}(\sqrt{a}\xi)}, \tag{15}$$

where a and b are given by (10). Figure 1 shows the profile of bright solitary-wave solution $v_1(x,0)$ for several different model coefficients which satisfy the constraint, i. e., $a>0$. In general, as the strength of the higher nonlinear terms, i. e., γ and δ increases, the width and amplitude of the solitary-wave also increases. Similar profiles for $v_2(x,0)$ are plotted in Fig. 2, however under the constraint $\sqrt{b^2-4ac}>0$ or equivalently $\gamma>\sqrt{4\beta\delta}$. It should be noted that for $\xi\to\pm\infty$, $v_{1,2}(\xi)$ has a non-zero background. This can be made to zero at infinity by imposing additional constraints on $\alpha,\beta,\gamma,\delta$, and λ.

3. Numerical Simulations

In this section, we numerically integrate (1) to understand the stability and dynamics of the solitary-wave solutions discussed in Section 2. Here "stability" means that the analytic solitary-wave preserves,

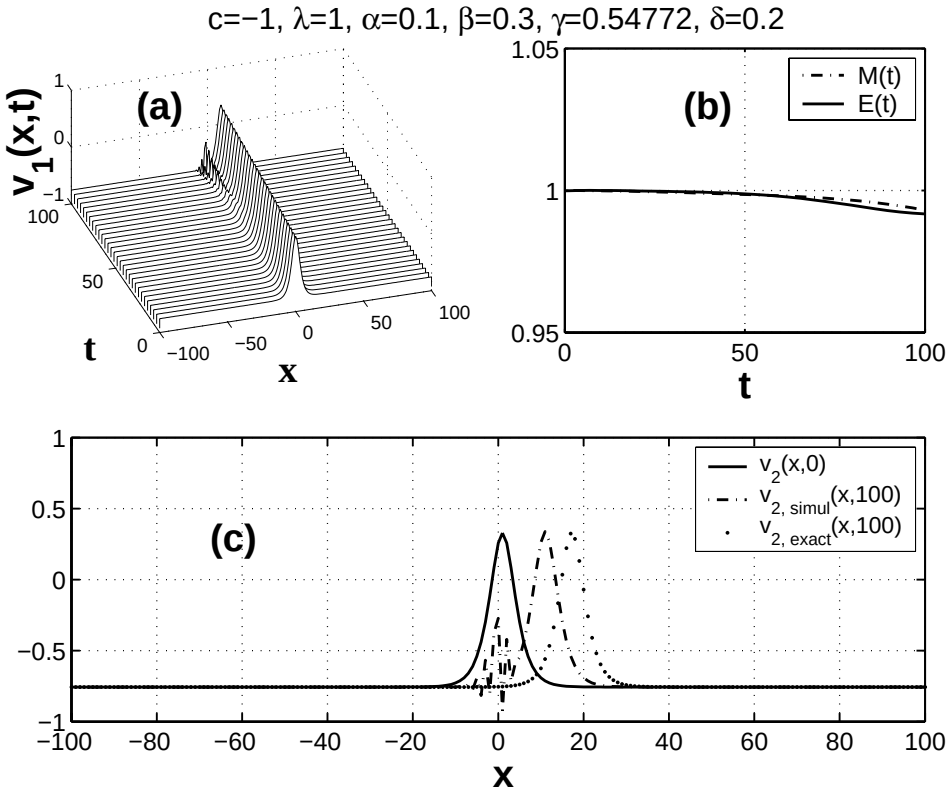

Fig. 4. a) Time evolution of numerically simulated $v_2(x,t)$. b) Exponentially increasing deviation from the initial values of the normalized mass and energy $M(t)$ and $E(t)$, respectively, indicates the instability of solitary-wave. c) Comparison of the numerically simulated wave profile at $t = 20$ with that of the exact solitary-wave solution in (14), showing unstable propagation along the evolution time, by emitting radiation in form of an oscillating tail.

when it is substituted in (1) and numerically integrated, its initial profile for a long propagation time without losing its energy by radiation. The numerical scheme used in this work is based on the time advance using the Runge-Kutta fourth-order scheme and a pseudo-spectral method using the discrete fast Fourier transformation in the spatial discretization [9], applying periodic boundary conditions. The numerical errors in the spatial discretization were controlled by varying the number of discrete Fourier modes between 128 and 1024 and various time steps between 10^{-5} and 10^{-3}.

In the following, we first investigate the stability of the solitary-wave solutions, for example, $v_1(x,0)$ and $v_2(x,0)$, by taking the initial profiles in the form

$$v_{1,2}(x,0) = \frac{-\gamma + \sqrt{\gamma^2 - 4\delta\beta}}{2\delta} - \frac{\sqrt{-2\delta c(\alpha+\lambda^2)}}{\delta}\chi_{1,2}(x),$$

$$\chi_1(x) = \frac{ab\,\mathrm{sech}^2(\frac{\sqrt{a}}{2}x)}{b^2 - ac[1-\tanh(\frac{\sqrt{a}}{2}x)]^2},$$
$$\chi_2(x) = \frac{2a\,\mathrm{sech}(\sqrt{a}x)}{\sqrt{b^2-4ac} - b\,\mathrm{sech}(\sqrt{a}x)}. \quad (16)$$

Before proceeding, we note that (1) is in general a non-integrable equation, because it is not certain whether the equation is satisfied by an infinity of time-independent integrals of motion. However, as at least the fundamental solitary-wave solutions indeed exists, we define the simplest two such integrals, namely the normalized mass and energy, as

$$M(t) = \int_{-\infty}^{\infty} v(x,t)\mathrm{d}x \Big/ \int_{-\infty}^{\infty} v(x,0)\mathrm{d}x \quad (17)$$

and

$$E(t) = \int_{-\infty}^{\infty} v(x,t)^2\mathrm{d}x \Big/ \int_{-\infty}^{\infty} v(x,0)^2\mathrm{d}x, \quad (18)$$

to further understand the dynamics of the waves.

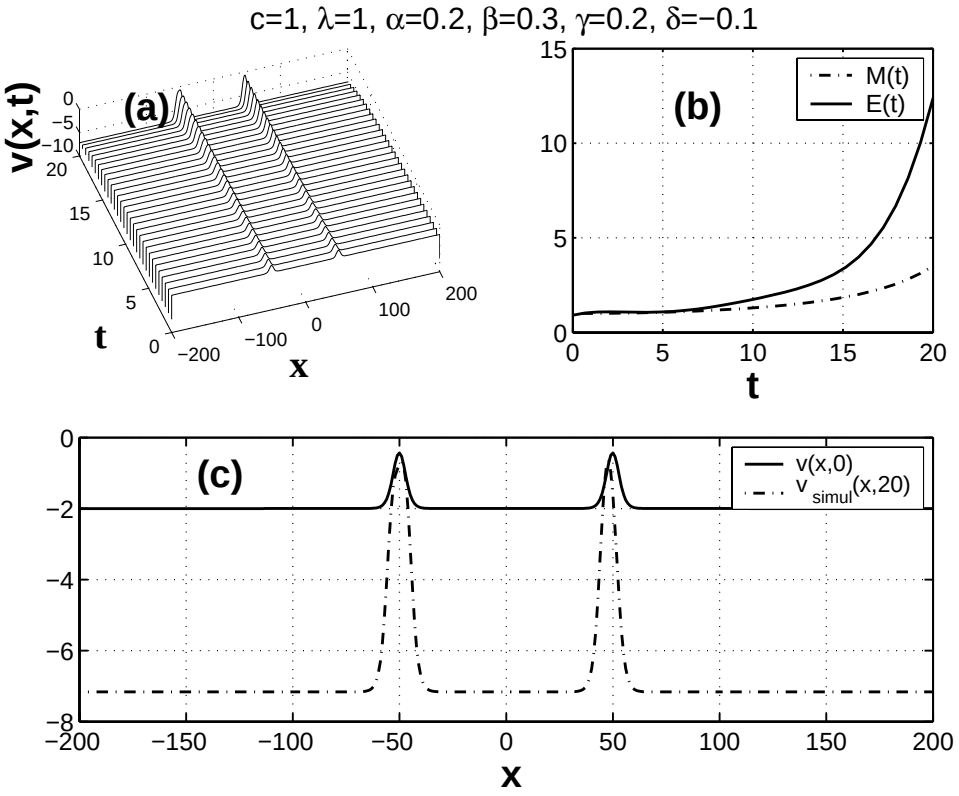

Fig. 5. a) Interaction dynamics of two solitary-waves with the initial profile as $v_1(x+\eta)+v_1(x-\eta)$, where $\eta = 50$ under the same coefficients as Figure 3. At beginning, the waves do not interfere each other but the amplitudes rapidly increase after $t \approx 8$ due to the interaction. b) The interaction process is 'totally inelastic' in the sense that $M(t)$ and $E(t)$ exponentially increase. c) Snapshot of the solitary-waves at $t = 20$ (dot-dashed curve), showing rapidly increasing amplitude.

Figure 3a shows the evolution of the bright solitary-wave $v_1(x,t)$ for the coefficients belonging to Figure 1. From Fig. 3b we can conclude that the solitary-wave is stable as both $M(t)$ and $E(t)$ are conserved, which indicates that the radiation loss due to the higher-order nonlinear terms is negligible since they are balanced by the dispersion term v_{xx} in (1). The accuracy of the numerical scheme in this work is also clearly demonstrated in Fig. 3c by comparing the exact analytic solution $v_{1,\text{exact}}(x,100)$ (dotted curve) with $v_{1,\text{simul}}(x,100)$ (dot-dashed curve).

In Fig. 4, we simulate the propagation of $v_2(x,t)$ for the set of coefficients in Figure 2. In comparison to the propagation of $v_1(x,t)$, the solitary-wave in this case emits radiation, as depicted in Fig. 4a, and becomes unstable after $t \approx 80$, at which both $M(t)$ and $E(t)$ decrease gradually, as shown in Figure 4b. It was confirmed by further numerical simulations that for all sets of coefficients in Fig. 2 the solitary-wave behavior of $v_2(x,t)$ is destroyed after $t \approx 120$ by emitting radiation in form of an oscillating tail. This radiation process acts as an effective friction, so that the speed of the solitary-wave decreases along its propagation, which can be clearly seen in Fig. 4c by comparing the simulated profile $v_{2,\text{simul}}$ (dot-dashed curve) with $v_{2,\text{exact}}$ (dotted curve).

As $v_1(x,t)$ is stable during its propagation, we would like to know its interaction dynamics with the initial profiles

$$v(x) = v_1(x+\eta)+v_1(x-\eta), \tag{19}$$

where η is the separation between the solitary-waves. By using the same set of coefficients as in Fig. 2, the interaction dynamics of the solitary-waves separated by $\eta = 50$ is simulated in Figure 5. At the beginning, as shown in Fig. 5a, the solitary-waves do not influence each other. They start to interact after $t \approx 8$, as can

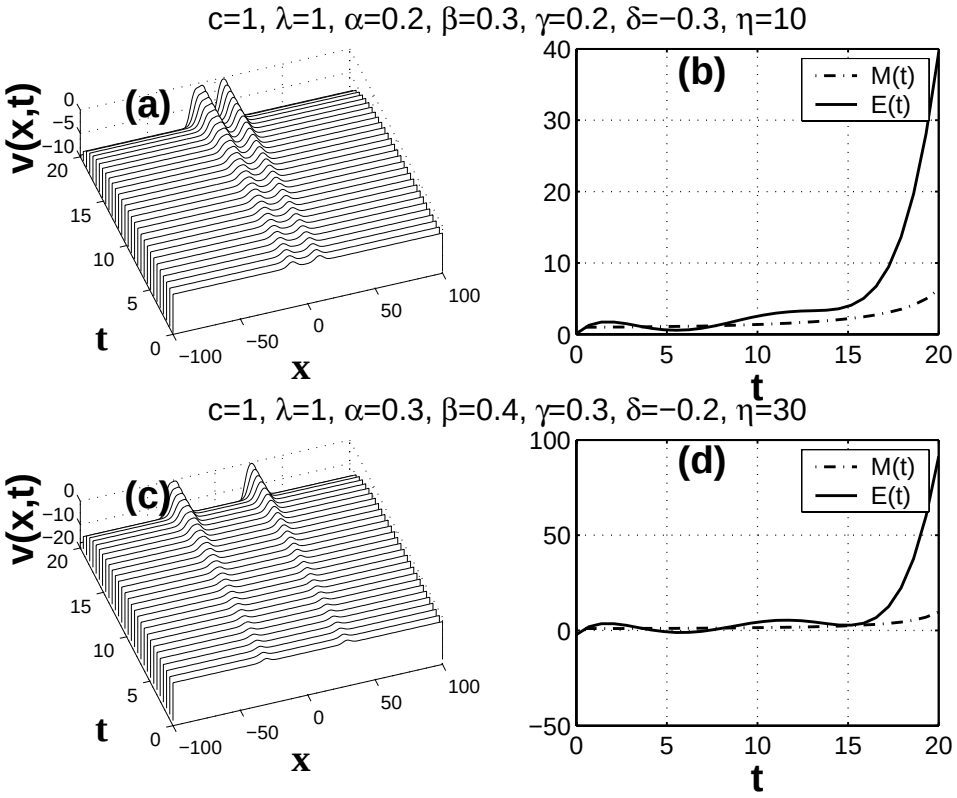

Fig. 6. a) and b) The time evolution of two solitary-waves with the initial separation $\eta = 10$ with the same coefficients as Fig. 5, exept $\delta = -0.3$. c) and d) The time evolution of two solitary-waves with initial separation $\eta = 30$ with a different set of coefficients. For both cases, the amplitudes rapidly increase regardless of the separation distance η or the strength of the coefficients.

be seen from the variations of $M(t)$ and $E(t)$ in Figure 5b. Their amplitudes rapidly grow along the time evolution. From Fig. 5b we observe that the whole interaction process is 'totally inelastic' in the sense that both $E(t)$ and $M(t)$ exponentially increase from the initial values owing to the presence of the higher-order nonlinear terms, which can not be balanced with the strength of the dispersion term, i. e., v_{xx}. After many simulations, we conclude that the amplitudes rapidly increase regardless of the separation distance η or the strength of the coefficients, as shown in Figs. 6a – b for $\eta = 10$ with the same coefficients as in Fig. 5, except $\delta = -0.3$. Figures 6c – d shows for the case $\eta = 30$ with a different set of coefficients. In contrast to the stable propagation of the single solitary-wave in Fig. 5, the presence of nonlinear terms for the interaction process of the two solitary-waves seems to act as a driving force for the system.

4. Conclusions

In this work, we have found new analytic solitary-waves, having nonzero background at infinity, of the generalized reaction-Duffing model [4, 6], by utilizing auxiliary equation method [7, 8]. The eight solitary-wave solutions according to (10) – (13), (8) and (6), exist under the two types of constraints, i.e, $a > 0$ or $a > 0$ and $\sqrt{b^2 - 4ac}$, respectively, from which the model coefficients $\alpha, \beta, \gamma, \delta$, and the wave number λ can be further constrained. We have shown by numerical simulations, for example, the dynamics of the two types of solitary-wave solutions in (14) and (15). It has been shown that, depending on the sign and strength of nonlinear coefficients in (1), the solitary-wave solutions can be stable or unstable along their evolutions, as shown in Figures 3 – 4. By taking the two stable solitary-waves as initial profiles, we have shown that the amplitudes rapidly increase, regardless of the sepa-

ration distance η or the strength of the coefficients, as shown in Figures 5 – 6.

Acknowledgement

We thanks the anonymous referee for his/her valuable comments and prompt review. This research was supported by the Catholic University of Daegu in 2004.

[1] D. Zwinllinger, Handbook of Differential Equations, Academic Press, London 1989.
[2] C. Gu et al., Soliton Theory and Its Application, Zhejiang Sci. Tech. Press, Hangzhou 1990.
[3] M. Ablowitz et al., Soliton, Nonlinear Evolution Equations and Inverse Scattering, Cambridge Univ. Press, Cambridge 1991.
[4] Z. Y. Yan and H. Zhang, Comm. Non. Sci. and Num. Sim. **4**, 224 (1999).
[5] T. Xia, H. Zhang, and Z. Y. Yan, Appl. Math. and Mech. **22**, 788 (2001).
[6] B. Tian and Y. T. Gao, Z. Naturforsch. **57a**, 39 (1999).
[7] E. V. Krishnan, J. Math. Phys. **31** 1155 (1990).
[8] E. Yomba, Chaos, Solitons and Fractals, **21** 75 (2004).
[9] L. N. Trefethen, Spectral Method in Matlab (Siam, 2000).